BNL-101878-2014-TECH
AD/RHIC/RD/95;BNL-101878-2013-IR

The Coupling Impedance of the RHIC Injection Kicker

H. Hahn

September 1995

Collider Accelerator Department
Brookhaven National Laboratory

U.S. Department of Energy
USDOE Office of Science (SC)

DISCLAIMER

AD/RHIC/RD–95

RHIC PROJECT

Brookhaven National Laboratory

The Coupling Impedance of the RHIC Injection Kicker

H. Hahn, M. Morvillo and A. Ratti

September 1995

THE COUPLING IMPEDANCE OF THE RHIC INJECTION KICKER

H. Hahn, M. Morvillo and A. Ratti

I. Introduction

The RHIC injection kicker is configured as a "C" cross section magnet with interspersed ferrite and dielectric bricks to approximate a transmission line as shown in Fig. 1. The dielectric bricks replace the lumped capacitors used in the more conventional plate kicker configurations used at other laboratories. This solution was suggested by Cassel[1] as an economical way of building a transmission line kicker and adopted by Forsyth et al[2] in order to achieve the required 95 nsec (1 - 99%) risetime. The use of ceramic bricks with a relative dielectric constant of ~100 provides the capacitance missing in the original slab ferrite constructions[3] and which now results in a true transmission line kicker. The high dielectric constant entails, however, the danger of high local electric stress, potentially limiting the peak field achievable. Another peculiarity of this solution was observed by Mane et al[4] in the measurement of the longitudinal coupling impedance, which exhibits sharp resonances in the GHz region.

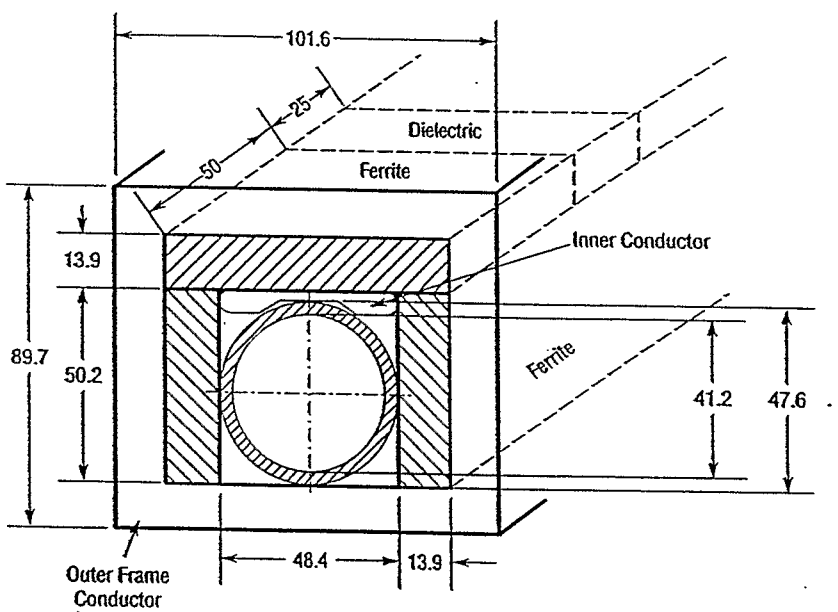

Fig. 1. RHIC Injection Kicker Geometry

[1] R. Cassel, private communication, 1992.
[2] E. B. Forsyth, G. C. Pappas, J. E. Tuozzola and W. Zhang, PAC Dallas 1995.
[3] R. Cassel, A. Donaldson, T. Mattison, G. Bowden, J. Weaver, F. Bulos, D. Fiander, Proc. IEEE Part. Acc. Conf., San Francisco, CA 1991, p. 996.
[4] V. Mane, S. Peggs. D. Trbojevic and W. Zhang, PAC, Dallas, TX 1995.

In response to the difficulties encountered, it was considered prudent to evaluate two alternative solutions:

- the "all-ferrite" kicker which is expected to allow higher peak fields at the expense of rise time and flatness of the pulse
- and a "hybrid" kicker in which dielectric bricks are used only above the inner conductor and are eliminated from the two sides and replaced with ferrite bricks. This maintains the transmission line character of the kicker but increases its characteristic impedance by ~10%. Improvements as to peak field can be expected but need confirmation.

As part of this evaluation, the coupling impedance of one each half-size ferrite-dielectric and all-ferrite kicker model was remeasured and the results are presented in this report. In summary, the total coupling impedance of the four full-size ferrite-dielectric kickers in one ring was found to be $Z/n = 0.16\ \Omega$/ring up to 1 GHz. The all-ferrite kicker has 0.13 Ω/ring with no resonances observable. Measurement of individual cells allows the conclusion that the hybrid kicker will have a coupling impedance essentially the same as the all-ferrite kicker. The resonances in the GHz region observed in the ferrite-dielectric kicker have been identified as resonances, localized in the dielectric bricks, which are decoupled from each other by the strong ferrite losses at the relevant frequencies.

The coupling impedance was measured using the wire method in which a resistive match provides a smooth transition from the 50 Ω of the network analyzer to the 165 Ω of the reference line in the setup.[5] The advantage of this method stems from the simplicity of its calibration procedure and the fact that a sufficient approximation of the results in terms of real/imaginary impedance or magnitude/phase is directly provided and can be plotted by the network analyzer without post processing. However, the results quoted above were obtained using the more accurate "log-formula"[6] appropriate for distributed systems. Details of the measurement method and its interpretation are found in Appendix I.

[5] A. Ratti, Fourth EPAC, London 1994, Vol. 2, p. 1262.
[6] L. S. Walling, D. E. McMurry, D. V. Neuffer, H. A. Thiessen, Nucl. Instr. Meth., A 281, p. 433 (1989).

II. The Ferrite-Dielectric Kicker

The forward scattering coefficient $S_{21\mathrm{DUT}}$ of the half-size ferrite-dielectric kicker model (normalized to the calibrated reference line with $S_{21\mathrm{ref}} = 1$) is shown in Fig. 2 for the frequency range from 300 kHz to 3 GHz. The resulting longitudinal coupling impedance is shown in Fig. 3, and with an expanded scale in Fig. 4. The curves are directly plotted from the network analyzer, and thus are obtained from the scattering coefficent as

$$Z = 2Z_{\mathrm{ref}}\left(1 - S_{21\mathrm{DUT}}\right)/S_{21\mathrm{DUT}}$$

with $Z_{\mathrm{ref}} = 165\ \Omega$. In Fig. 4, the corrected impedance values at select frequencies are marked as crosses and were calculated using the log-formulae,

$$Z = -2Z_{\mathrm{ref}}\ln S_{21\mathrm{DUT}}$$

or explicitly,

$$\mathrm{Re}Z = -2Z_{\mathrm{ref}}\ln|S_{21\mathrm{DUT}}|$$

$$\mathrm{Im}Z = -2Z_{\mathrm{ref}}\angle S_{21\mathrm{DUT}}$$

Using the corrected results, one finds for frequencies from ~ 0.1 to 1 GHz $Z/n = 20.2\ \mathrm{m}\Omega$ and for the four kicker units in one ring $0.162\ \Omega$, with the result independent of the kicker terminations, as seen from Fig. 5, where the uncorrected kicker impedance for "both ends open" and "both ends shorted" is compared.

At frequencies below ~100 MHz, the kicker terminations influence the results and a full study, including the feeder cables (up to 75 m long) with the thyratron switch and the $25\ \Omega$ termination, remains to be carried out. Results for the kicker open at both ends are shown in Fig. 6. The sharp resonance at $\sim$ 20 MHz was predicted by the transmission line analysis[7] and is due to the ferrite-dielectric cell structure having an inductance of 90 nH and capacitance of 150 pF per cell.

In normal operation, the kicker output end is terminated in its characteristic impedance of $Z_{\mathrm{C}} \sim 25\ \Omega$. An upper-limit estimate of its coupling impedance is obtained from the kicker terminated at the output end and open at the input with the result shown in Fig. 7.

In an attempt to correlate measurements with the frequently quoted, theoretical predictions by Nassibian,[8] the $\ell = 0.5$ m long kicker model was measured with both ends terminated in its characteristic impedance. The measured results shown in Fig. 8 differ significantly from the predictions. The first dip at 36.4 MHz in the resistive component of the impedance, which corresponds to $\kappa_{\mathrm{C}}\ell = 2\pi$ yields a propagation velocity of

$$\frac{v}{c} = \frac{f\ell}{c} = 0.06$$

in sufficient agreement with the measured propagation velocity, but the resistive peak of $6\ \Omega$ at $\kappa_{\mathrm{C}}\ \ell \sim \pi$ is only half the theoretical value which would imply a mutual coupling coefficient of only 0.25 instead of 0.5 as expected for a centered wire. This discrepancy is partially explained by the location of the wire, nominally at 20.6 mm above the bottom

[7] H. Hahn and E. B. Forsyth, Fourth EPAC, London 1994, Vol. 3, p. 2550.
[8] G. Nassibian, Report CERN/PS 84-25(BR), 1984.

plate, but sagging to 19 mm in the middle of the kicker, and displaced from the ideal center at 23.5 mm. Furthermore, one can assume that the beam couples to the kicker mostly through the ferrite bricks which cover only 2/3 of the axial length. However, at the frequency of 36.4 MHz, one would expect an inductive component of $Z = \pi Z_C/2 = 39\ \Omega$ versus the measure $\sim 9\ \Omega$. A factor of 2 could be explained with a smaller coupling coefficient, but the remaining factor of 2 requires a different explanation, possibly due to the non-ideal ferrite properties.

At frequencies above 1 GHz, the paramount feature of the results is the appearance of resonances at 1.02, 1.76, and 2.74 GHz. In order to verify the hypothesis that these resonances are caused by the dielectric cells, the coupling impedance of a single dielectric cell, 2.5 cm long in beam direction, was measured with the results in Fig. 9 clearly demonstrating the possibility of high-Q resonances. Subsequently, a combination of ferrite+dielectric+ferrite cells, 12.5 cm long, was measured with the result given in Fig. 10 showing resonances at 1.06, 1.86, and 2.84 GHz, in correspondance to the kicker frequencies. In a combination of 2 1/2 ferrite cells, with the same 12.5 cm length, the coupling impedance shown in Fig. 11 is in the GHz region resistive, and almost noninductive, with no resonances observed. (The small spikes are calibration errors as seen from Fig. 12 which shows the impedance of the setup alone, corrected to give $S_{21\mathrm{ref}} = 1$.)

In an additional test to identify the origin of the resonances, it was attempted to treat the entire kicker as a cavity and to excite resonances by loops. Only localized resonances (trapped modes ?) could be excited. It thus can be concluded that the kicker resonances are due to the sum of essentially separate dielectric cell resonances, which are decoupled by the lossy ferrite cells.

Anticipating the construction of a hybrid kicker, where dielectric bricks are only used in the top layer but not at the sides, a combination of ferrite+ ferrite dielectric hybrid+ferrite cells, 12.5 cm long, was tested. The results in Fig. 13 are almost identical to the all-ferrite combination and allow the prediction that the hybrid kicker will be free of resonances and have the same, lower Z/n as the all-ferrite kicker.

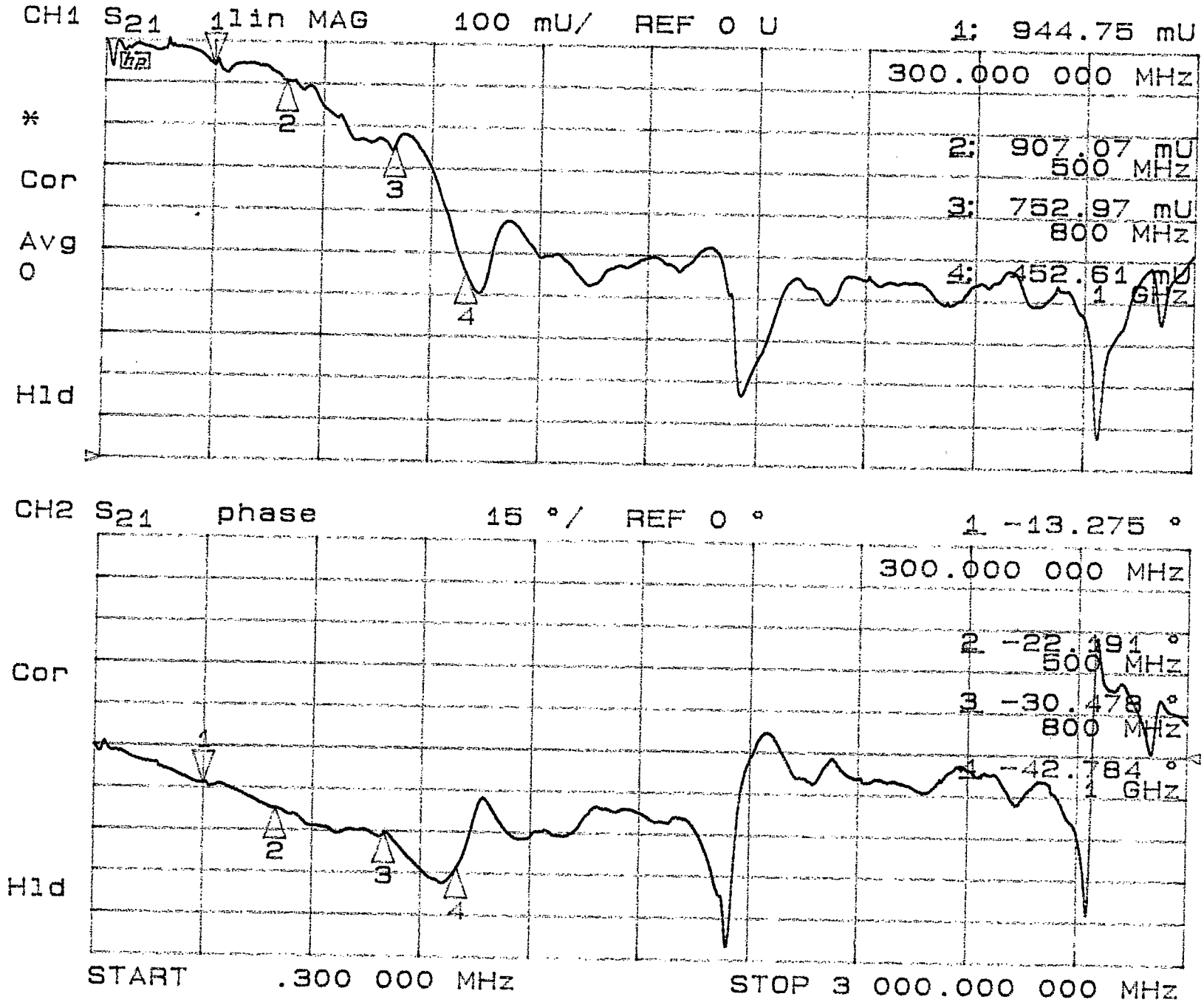

Fig. 2. Forward scattering coefficient of ferrite-dielectric kicker

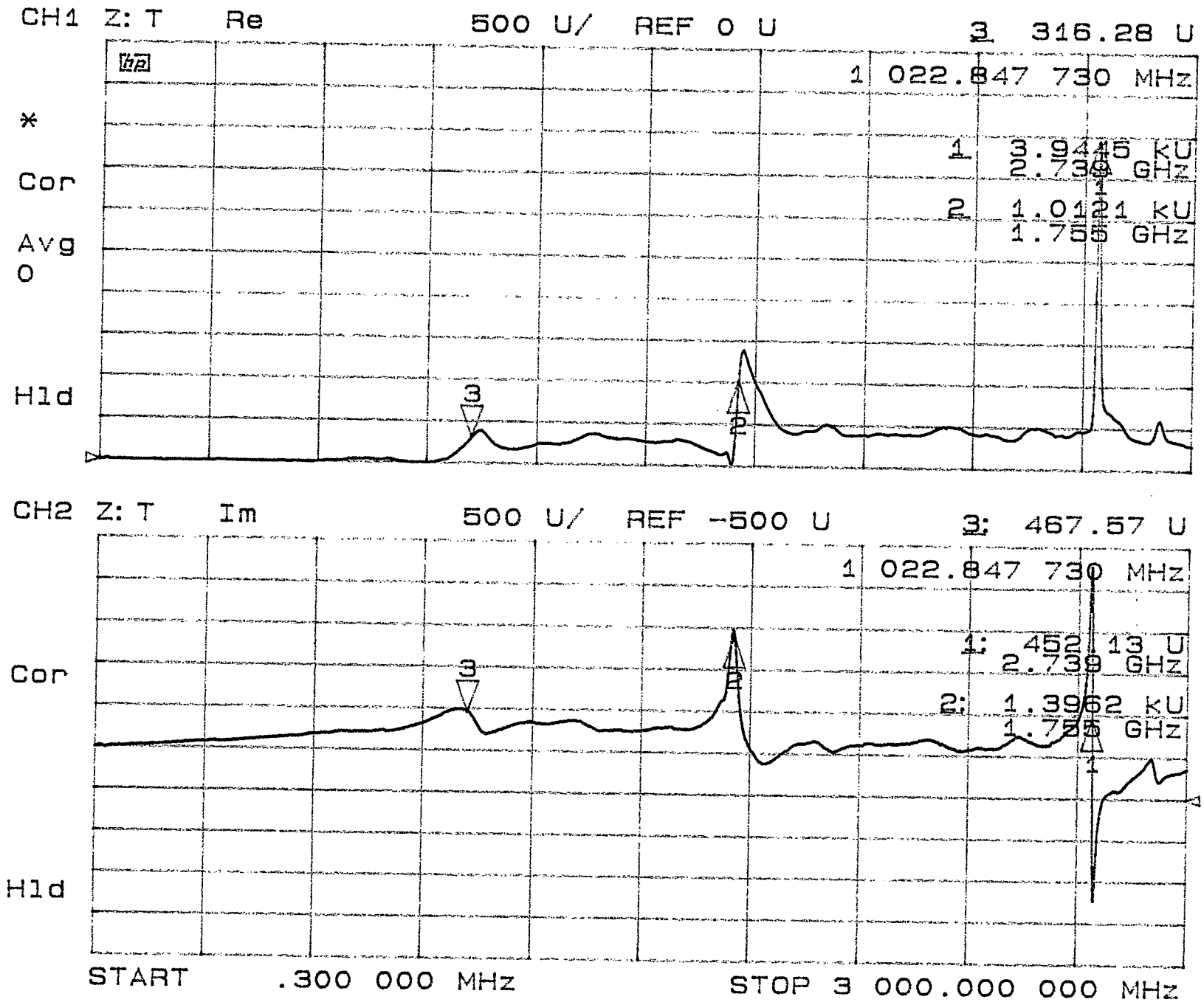

Fig. 3. Coupling impedance of ferrite-dielectric kicker

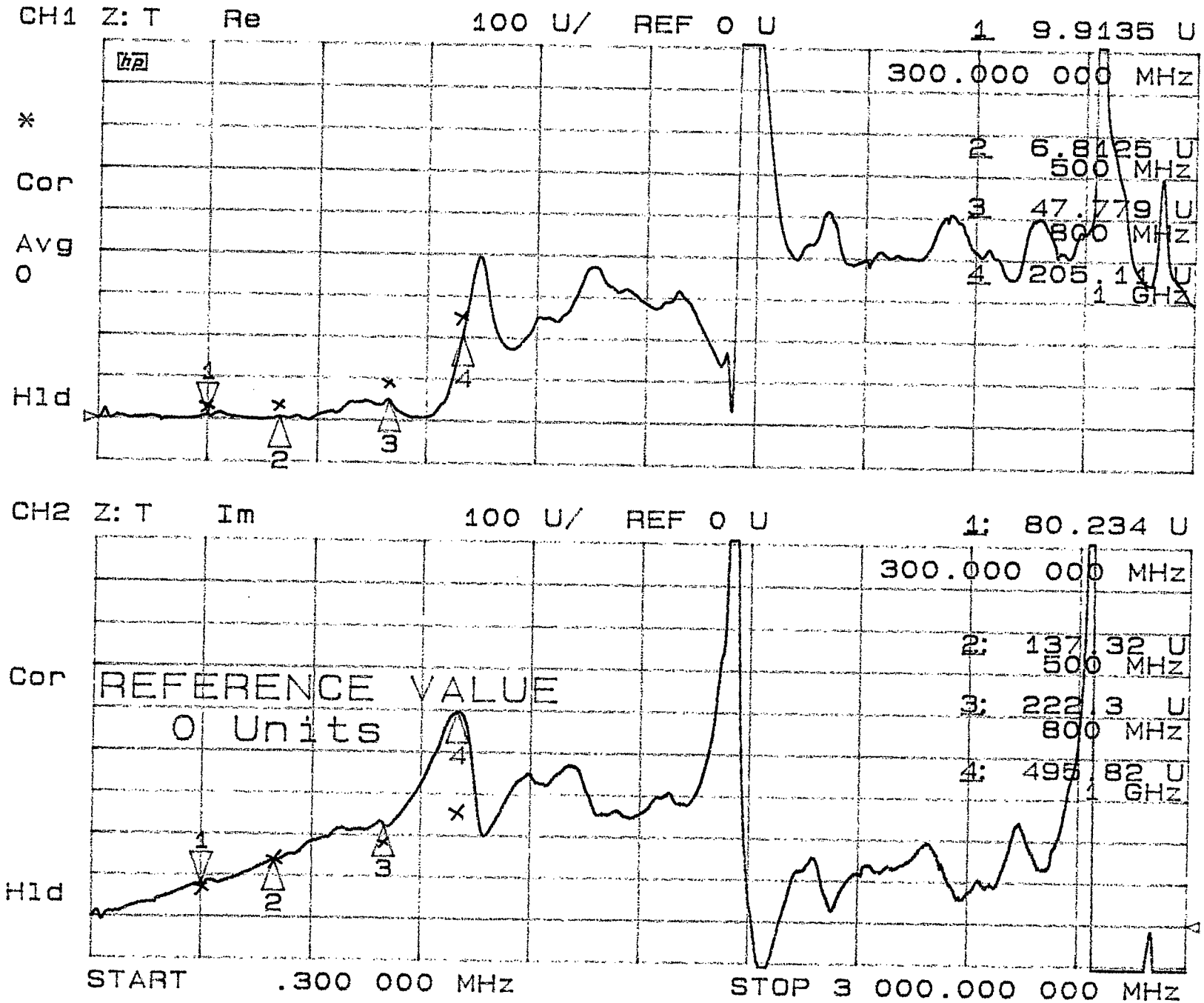

Fig. 4. Coupling impedance of ferrite-dielectric kicker
(X obtained with log-formula)

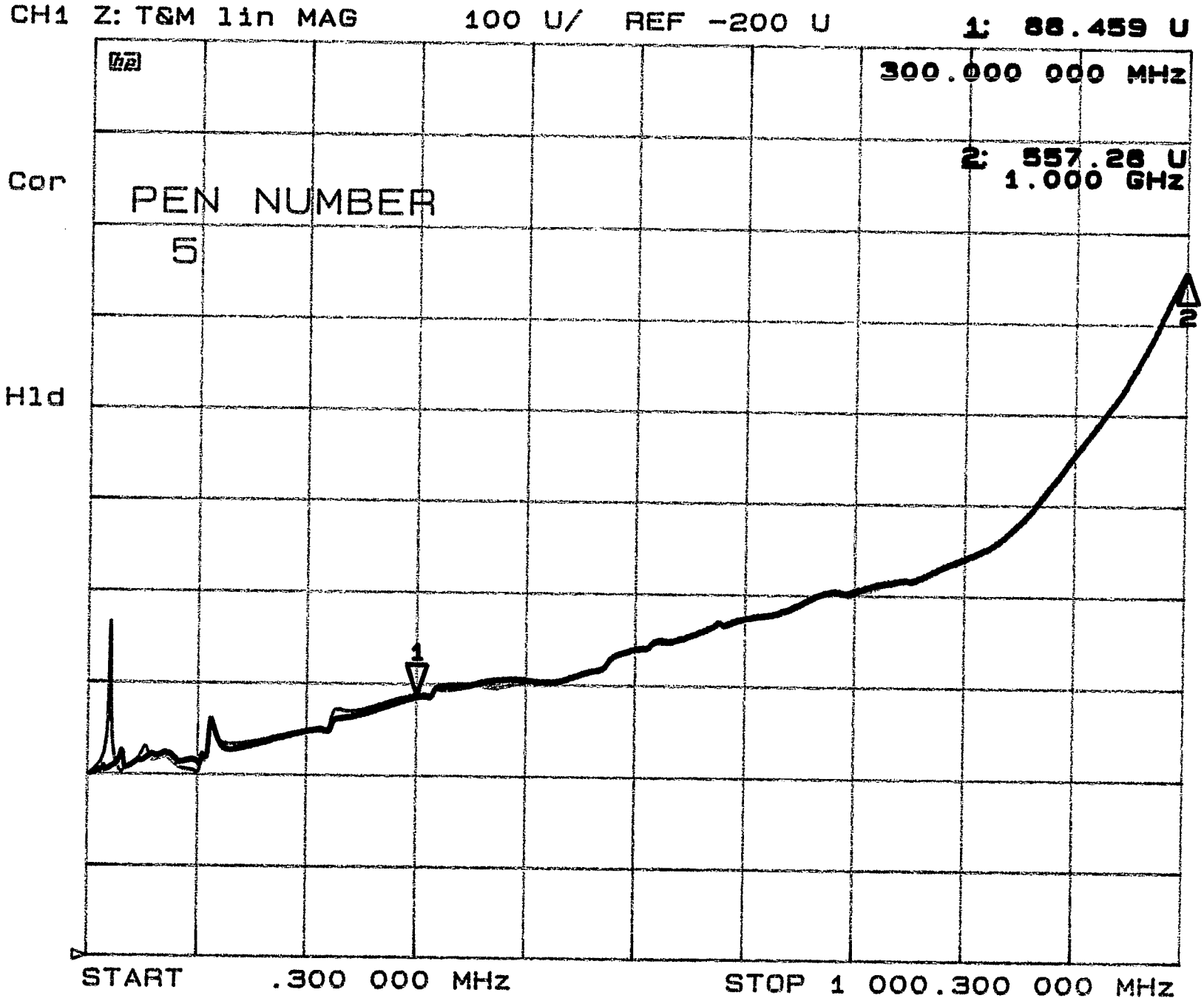

Fig. 5. Comparison of ferrite-dielectric kicker impedance with open and shorted ports

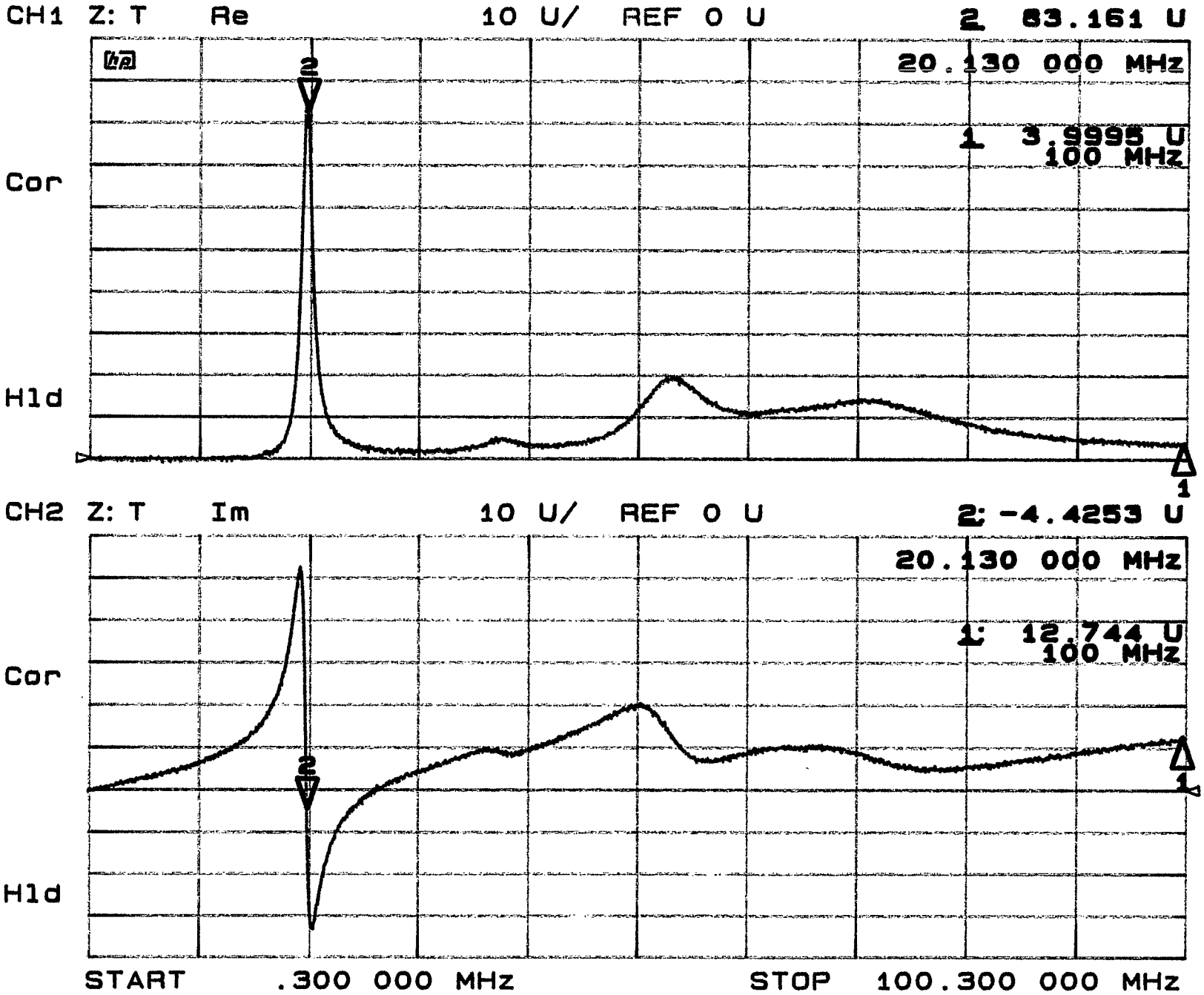

Fig. 6. Impedance of ferrite-dielectric kicker with both ports open

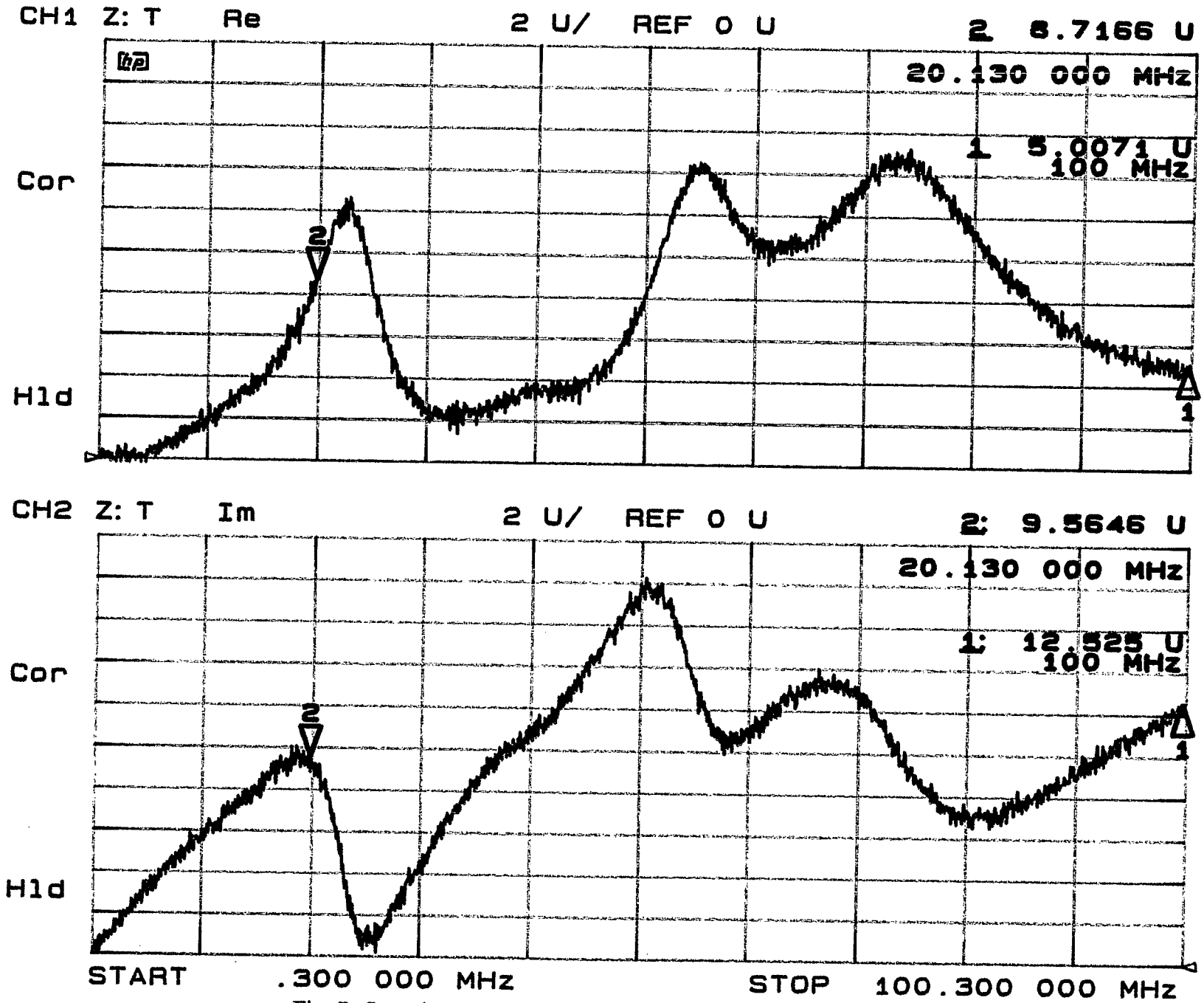

Fig. 7. Impedance of ferrite-dielectric kicker with input port open and output port terminated in 25 Ω

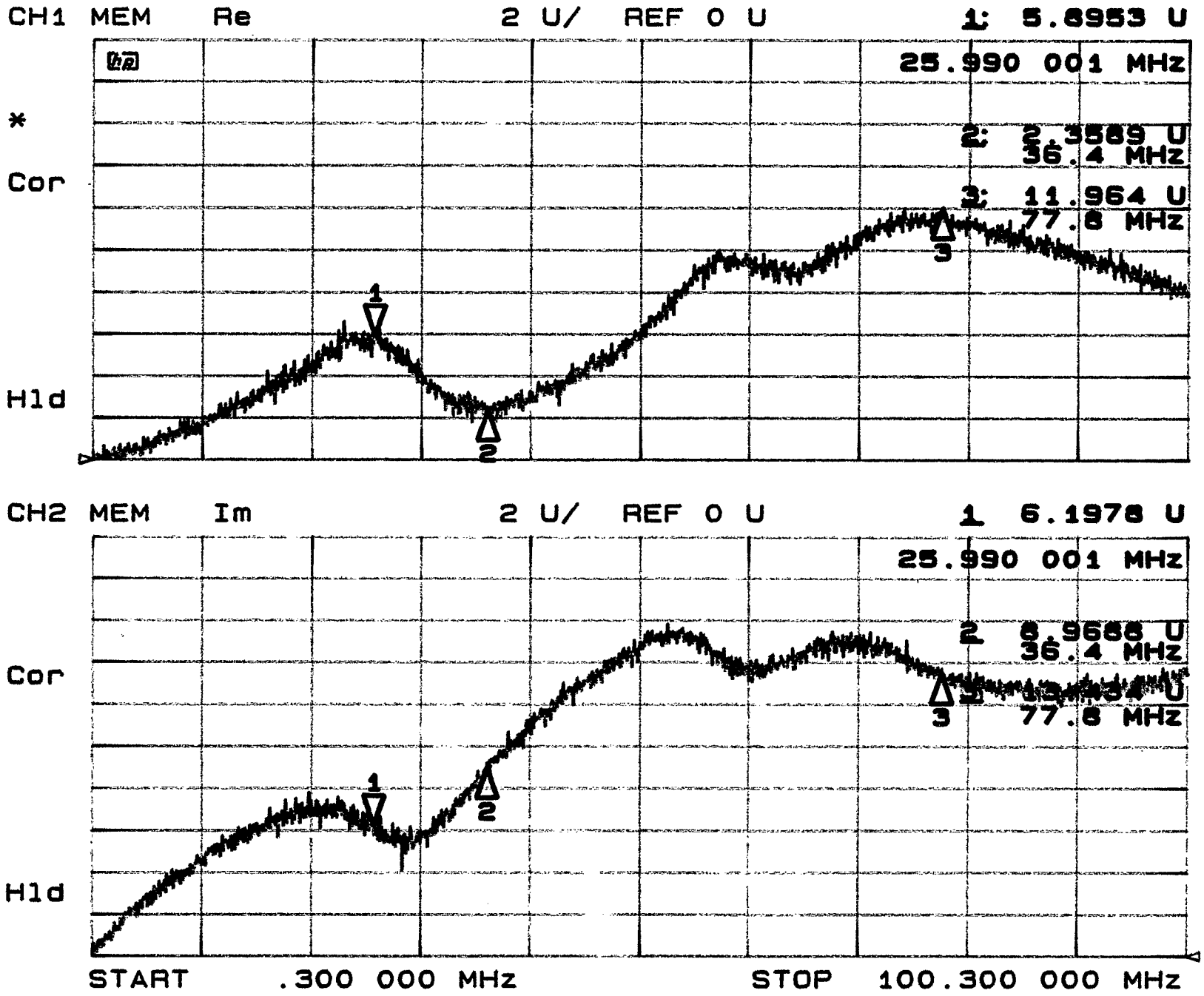

Fig. 8. Impedance of ferrite-dielectric kicker with input and output ports terminated in 25 Ω

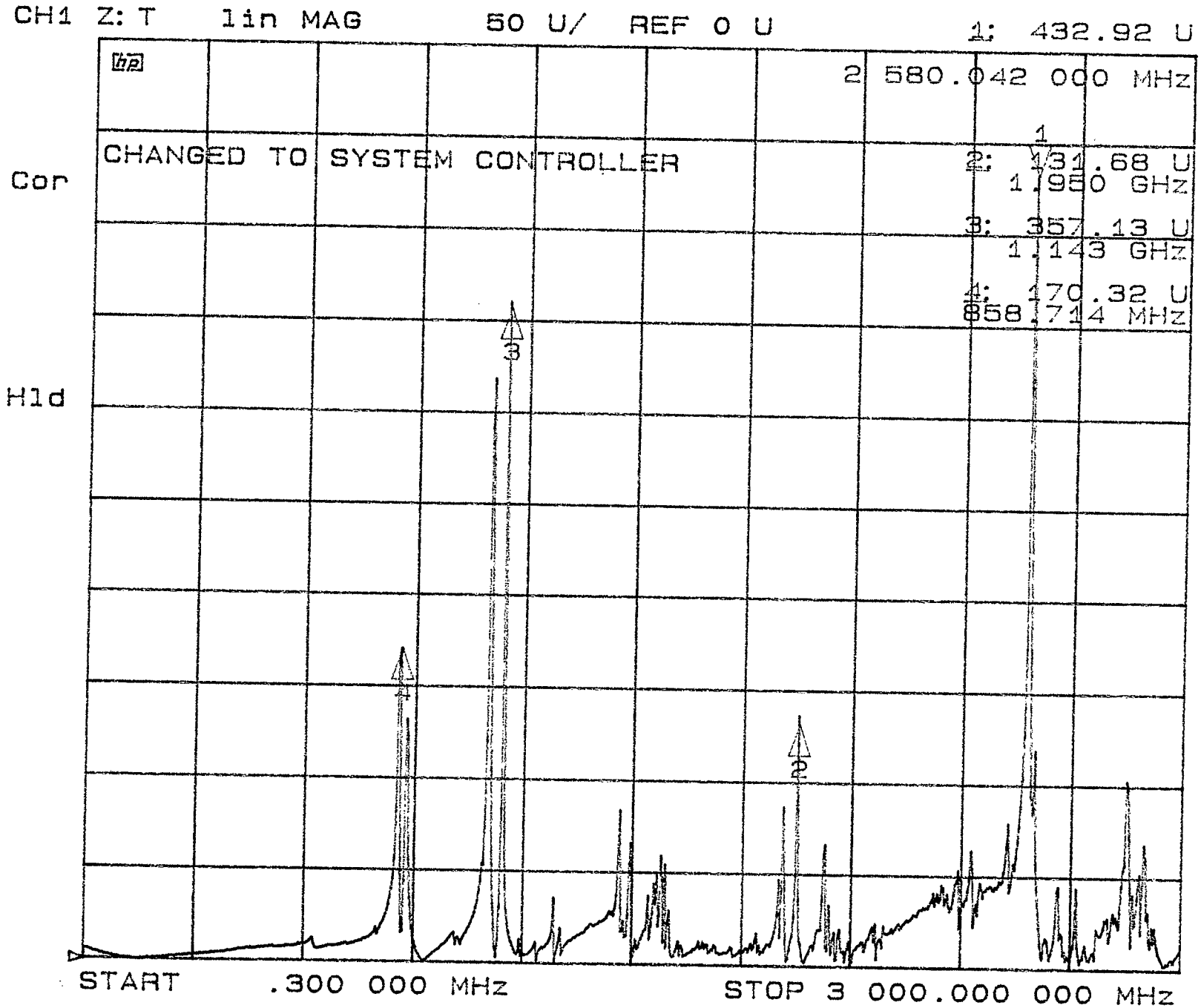

Fig. 9. Impedance of 1 dielectric cell (2.5 cm)

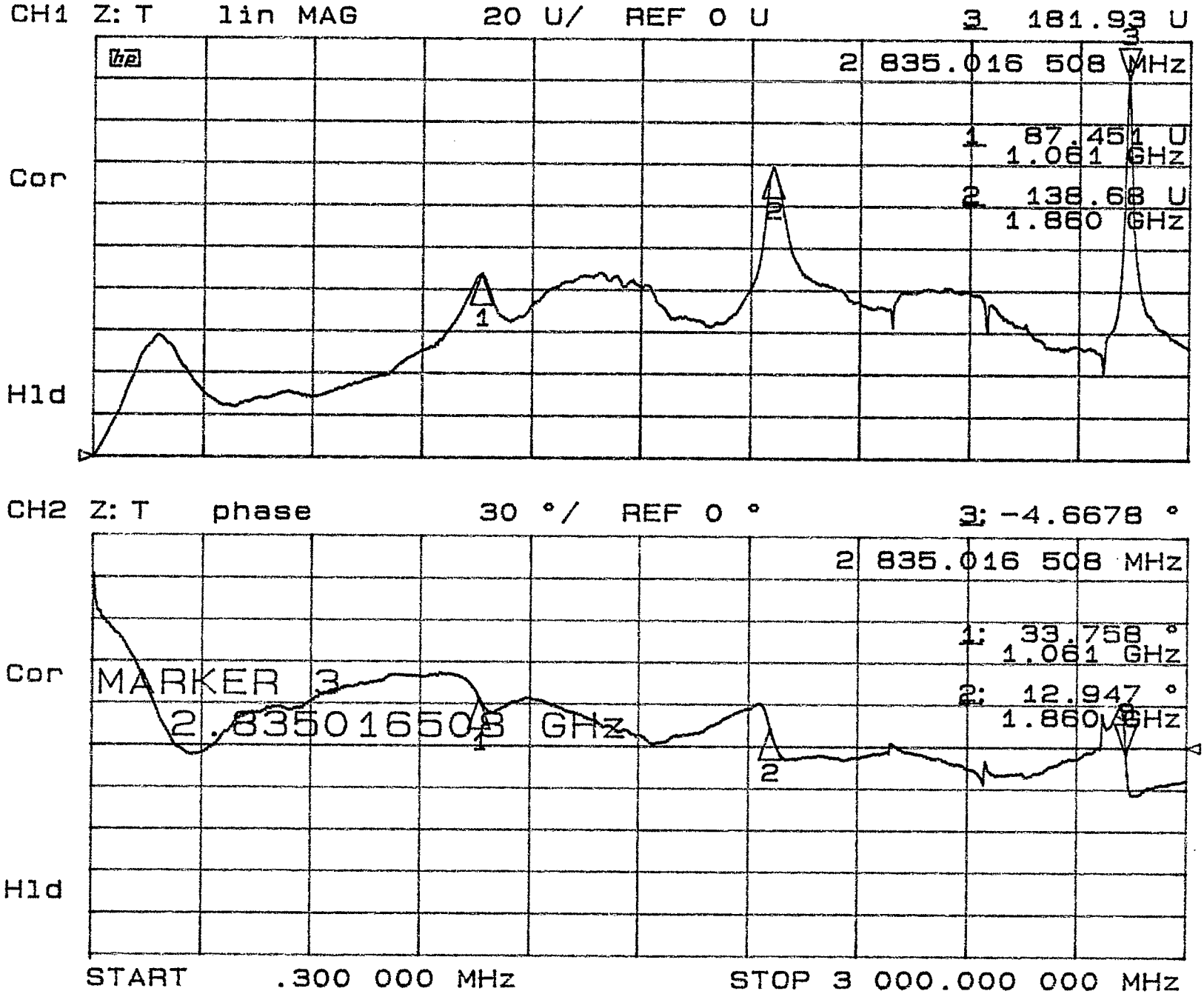

Fig. 10. Impedance of ferrite+dielectric+ferrite cells (12.5 cm)

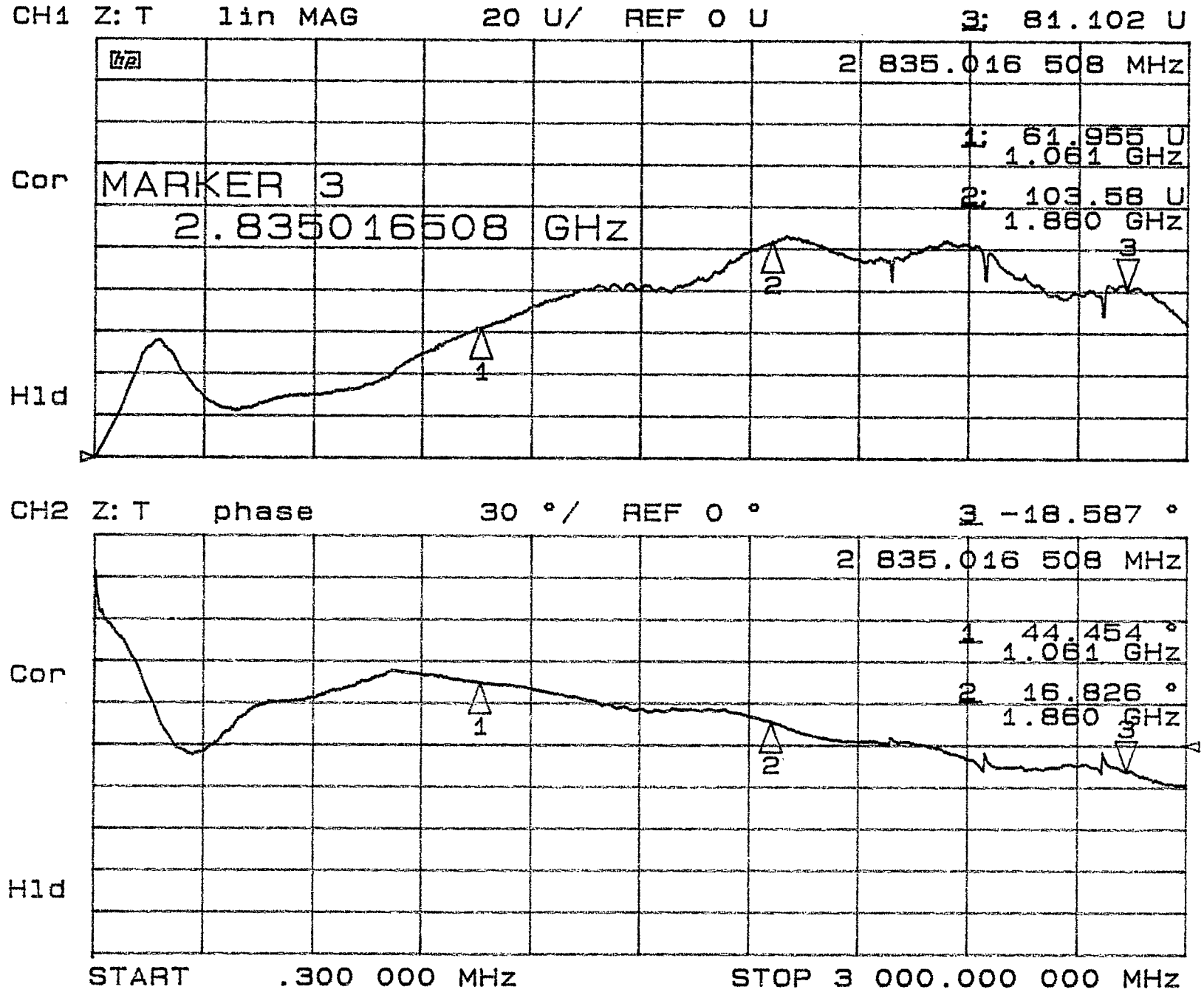

Fig. 11. Impedance of 2 ½ all-ferrite cells (12.5 cm)

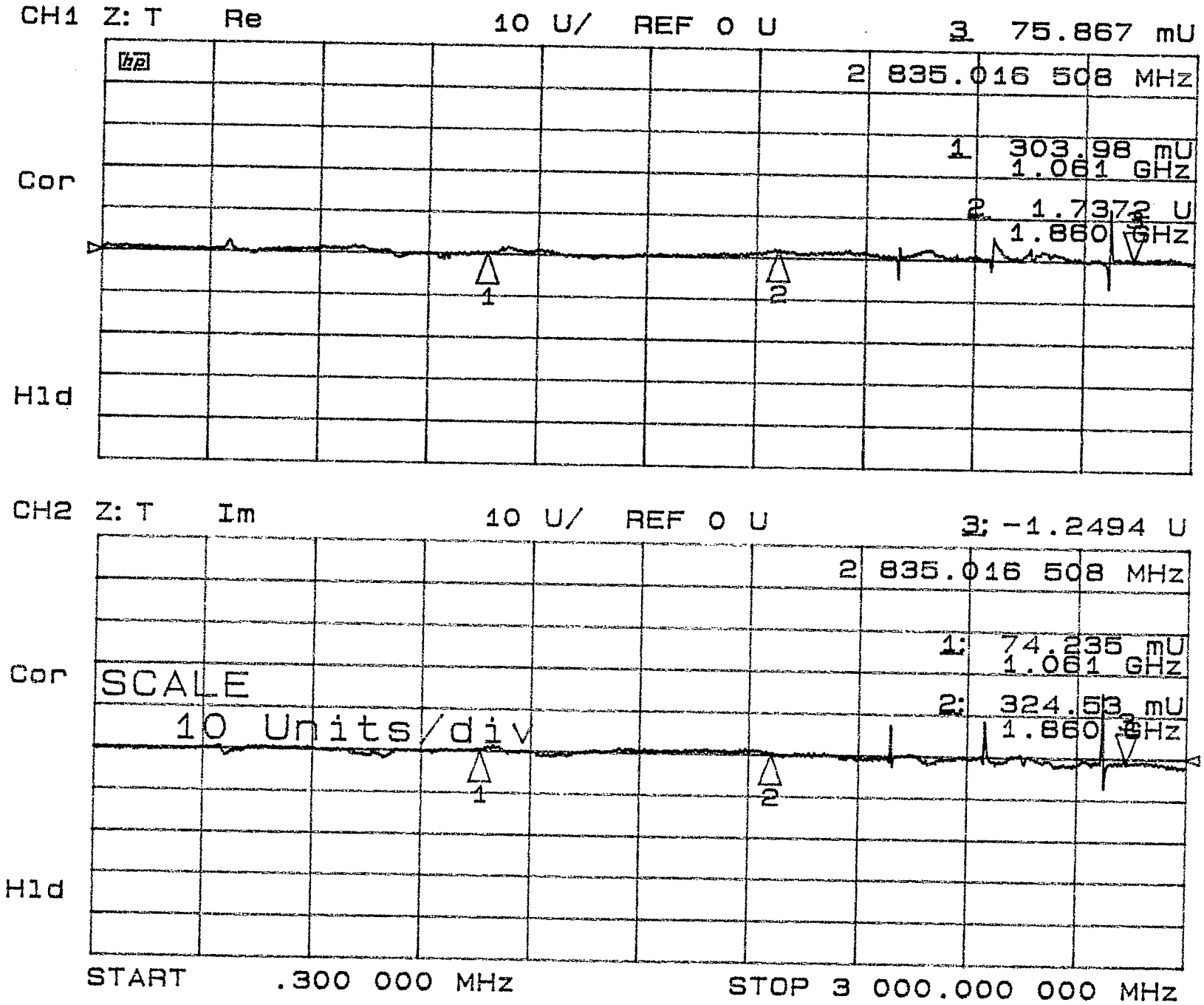

Fig. 12. Impedance of calibrated bench set up

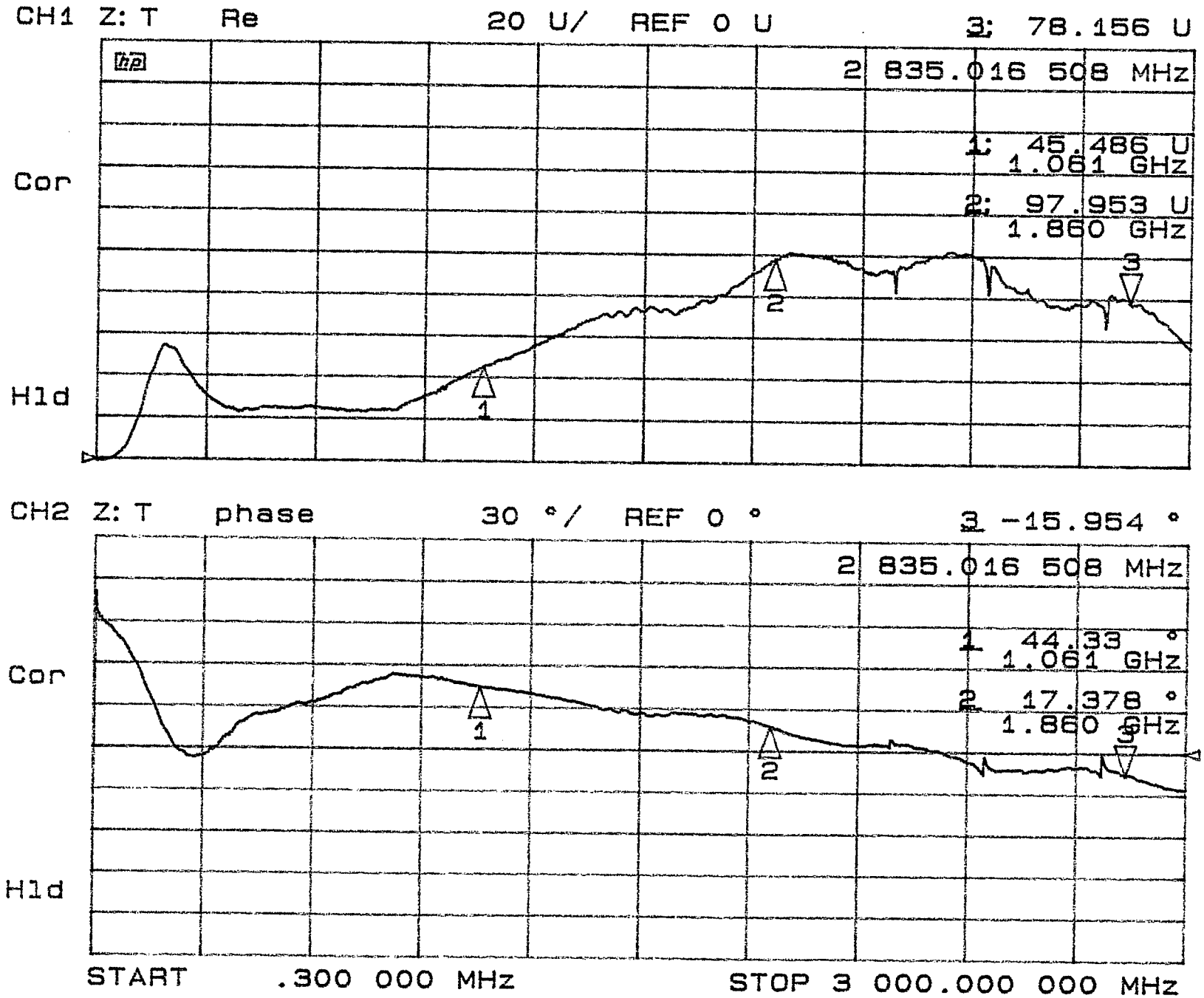

Fig. 13. Impedance of ferrite+hybrid+ferrite cells (12.5 cm)

III. The All-Ferrite Kicker

The forward scattering coefficient $S_{21\mathrm{DUT}}$ of the half-size all-ferrite kicker model is shown in Fig. 14 for the frequency range from 300 kHz to 3 GHz. The resulting longitudinal coupling impedance is shown in Fig. 15. The curves are directly plotted from the HP-network analyzer, but corrected values at selected frequencies are marked on the figure. Using the corrected results, one finds for frequencies from ~0.1 - 1 GHz a coupling impedance of $Z/n = 16.1$ mΩ for the half-length model and ~ 0.13 Ω per ring. In the GHz region, the coupling impedance is essentially resistive and Z/n decreases with n. As expected from the measurement of ferrite cells, no resonances are observed. A tentative explanation of this coupling impedance character as being an electric shock wave is given in Appendix II.

An upper-limit estimate of the coupling impedance below 100 MHz is obtained from the results in Fig. 16, with the input port open and the output port terminated with ~ 25 Ω (which is the characteristic impedance of the feeder cable in parallel but not of the "lumped-inductance" kicker).

Acknowledgements

It is a pleasure to acknowledge clarifying discussions and e-mail correspondence with Drs. Caspers and Dôme.

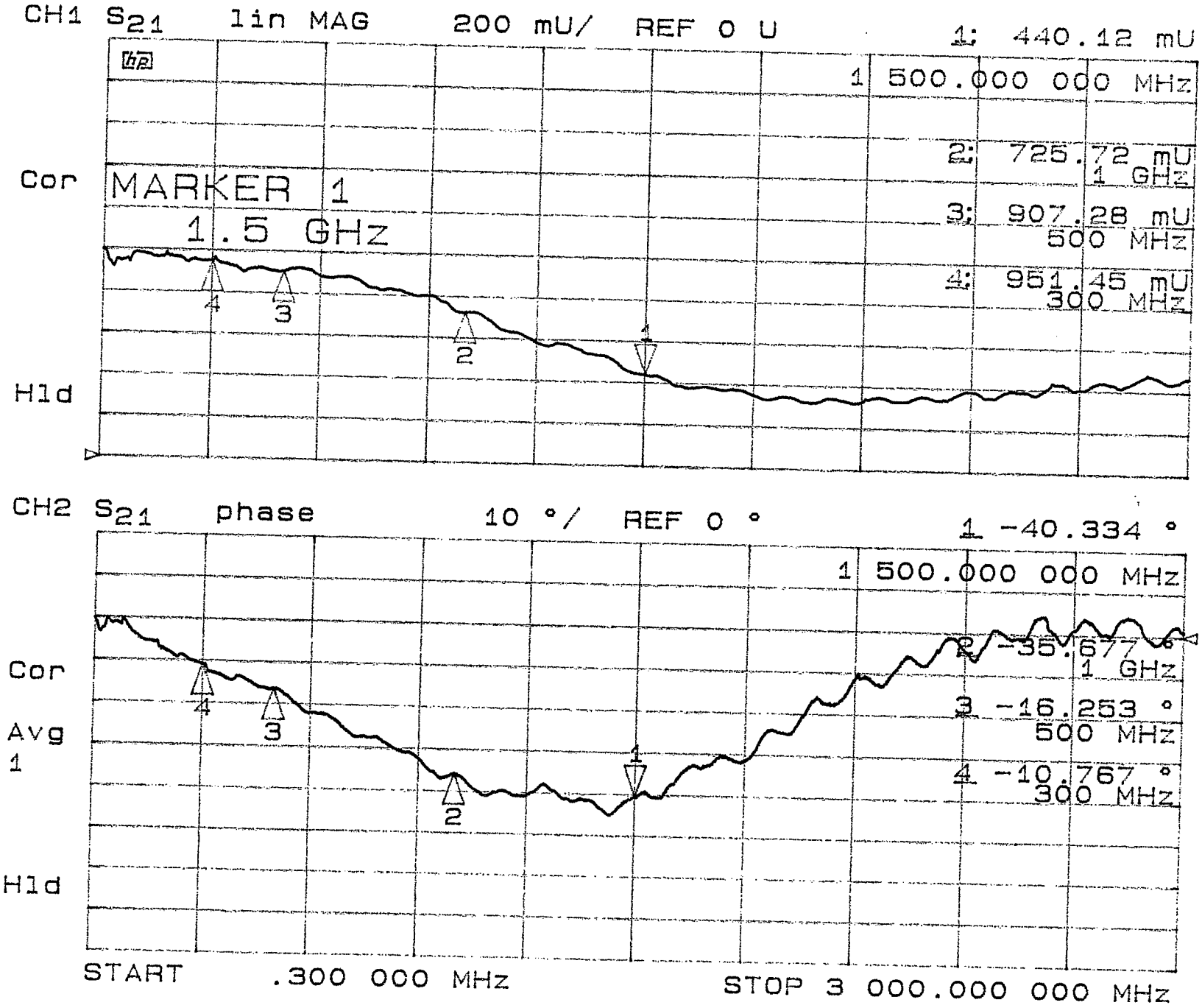

Fig. 14. Forward scattering coefficient of all-ferrite kicker

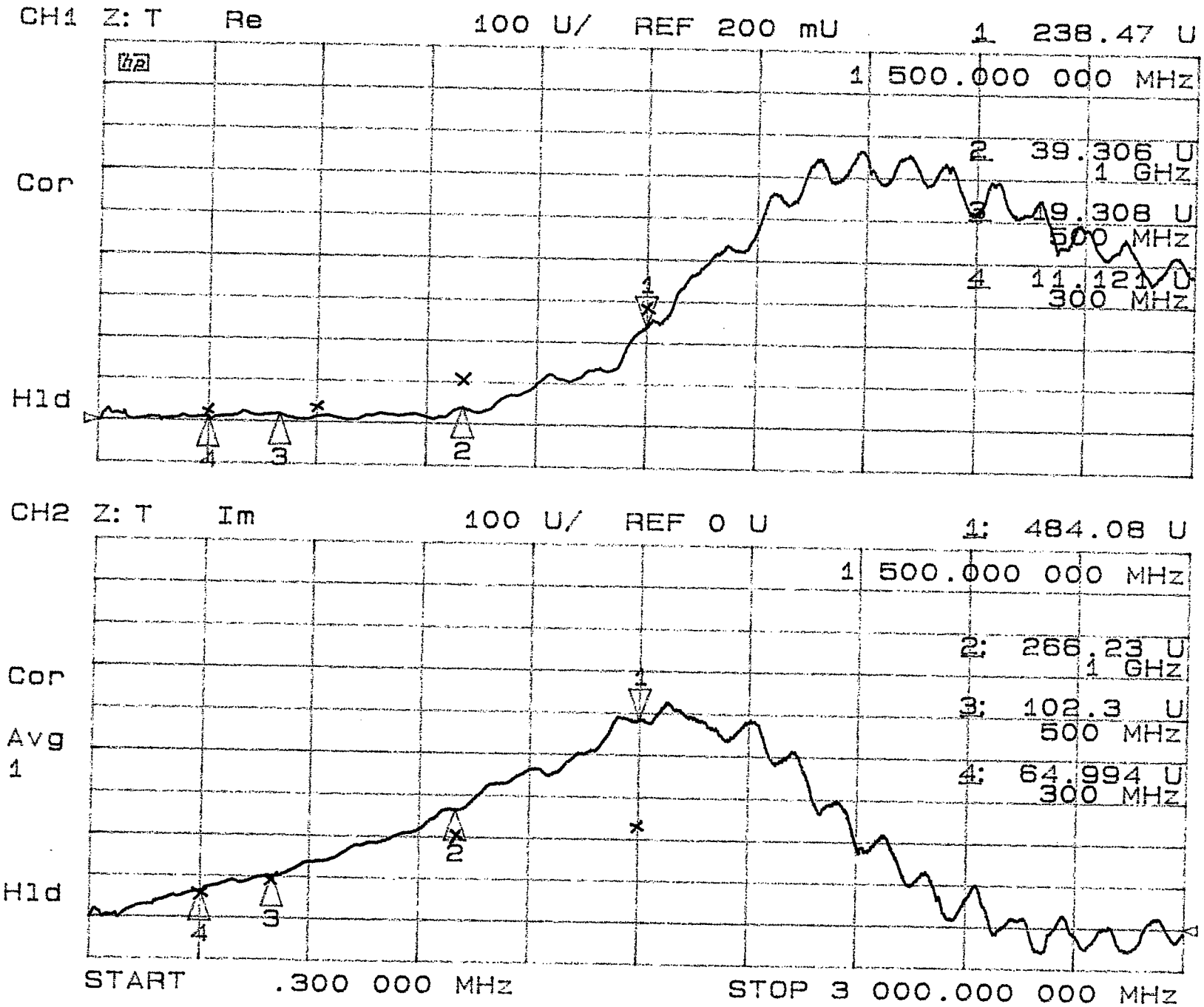

Fig. 15. Impedance of all-ferrite kicker

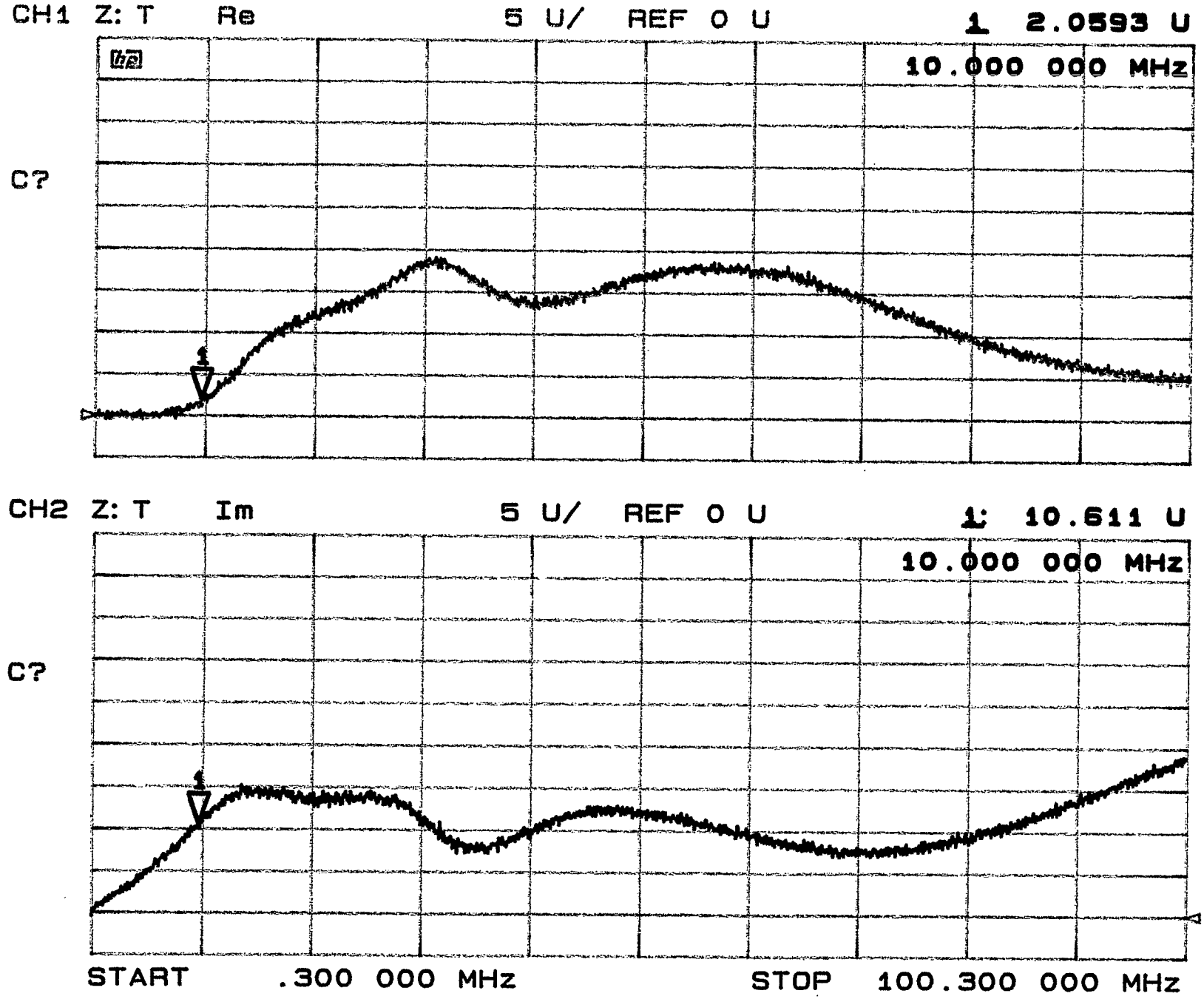

Fig. 16. Impedance of all-ferrite kicker with input port open and output terminated in 25 Ω

Appendix I: Wire Measurement of Distributed Impedances

The coupling impedance of the kicker models was measured with the existing bench setup for wire measurements used and described by Mane, et al.[4] However, significant changes were introduced, which made the interpretation of the results simpler and are believed to yield more accurate results.

The wire thickness was increased to 3.2 mm in order to avoid excessive sagging and increase the repeatability of results. The characteristic impedance of the wire in the rectangular pipe was measured directly to be $Z_{\rm ref} = 165\ \Omega$ by shorting the output port of the system and measuring the input impedance, $jZ_{\rm ref}\tan(\kappa_{\rm ref}\ell)$, with the Hewlett-Packard Network Analyzer 8753C connected to the S-Parameter Test Set 85078A.

The coupling impedance measurement of the "Device Under Test" was made using Ratti's implementation[5] of the wire method, in which a resistive match provides a smooth transition from the 50 Ω of the network analyzer to the 165 Ω of the reference line. The advantage of this method stems primarily from the simplicity of the "through reference" calibration procedure which allows on-line interpretation of the results and easy change of the frequency range covered. At the input port, a parallel resistor of $\sim$ 59.9 Ω and a series resistor of $\sim$ 137.7 Ω provides forward and backward matching. At the output port, a series resister of $\sim$ 115 Ω provides forward matching. The frequency dependence of the carbon resistors and stray inductances/capacitances destroys the match at higher frequencies, but is correctable by the calibration procedure. Further improvements can be achieved by gated measurements, which were applied in few cases.

The accuracy of the results was tested and confirmed by measuring the impedance of a 100 Ω carbon resistor shown in Fig. 17, which previously was calibrated by a measurement directly at the network analyzer input with the result given in Fig. 18. The measurements are considered accurate to $\pm$ 10% below 1 GHz, but become only qualitative above 2 GHz.

The coupling impedance measurement is obtained from the change in the forward scattering coefficient $S_{21\rm DUT}$ with respect to the reference measuring system with $S_{21\rm ref}$ (which by proper calibration can be made to be $S_{21\rm ref} = 1$). In the case of a single lumped disturbance, the coupling impedance is obtained by the well known formula[9]

$$Z = 2Z_{\rm ref}\frac{(1 - S_{21\rm DUT}/S_{21\rm ref})}{(S_{21\rm DUT}/S_{21\rm ref})}$$

This formula is also used by the hp Network Analyzer and is quite useful in an exploratory study involving distributed impedances. However, if accurate results are required, at least the "log-formula"[6] should be used; although itself an approximation, it is extremely simple to use and sufficient in the present application.

The general relation between the forward scattering coefficient and a distributed wall impedance is best obtained by field matching (i.e. voltage and current matching in a transmission line) which leads to the conditions (see Fig. 19):
- at the input port

$$a_{in} + b_{in} = a_{\rm DUT} + b_{\rm DUT}$$

$$\frac{1}{Z_0}(a_{in} - b_{in}) = \frac{1}{Z_{\rm DUT}}(a_{\rm DUT} - b_{\rm DUT})$$

[9] H. Hahn and F. Pedersen, Report BNL 50870 (1978).

- at the output port

$$a_{\mathrm{DUT}} e^{-j\kappa_{\mathrm{DUT}}\ell} + b_{\mathrm{DUT}} e^{j\kappa_{\mathrm{DUT}}\ell} = b_{out}$$

$$\frac{1}{Z_{\mathrm{DUT}}}\left(a_{\mathrm{DUT}} e^{-j\kappa_{\mathrm{DUT}}\ell} - b_{\mathrm{DUT}} e^{j\kappa_{\mathrm{DUT}}\ell}\right) = \frac{1}{Z_0} b_{out}$$

from which follows for the ratio of forward scattering coefficients

$$\frac{S_{21\mathrm{DUT}}}{S_{21\mathrm{ref}}} = \frac{4 Z_{\mathrm{DUT}} Z_0 e^{-j\kappa_{\mathrm{DUT}}\ell} e^{j\kappa_0\ell}}{\left(Z_{\mathrm{DUT}} + Z_0\right)^2 - \left(Z_{\mathrm{DUT}} - Z_0\right)^2 e^{-j2\kappa_{\mathrm{DUT}}\ell}}$$

with

$$Z_0 = Z_{\mathrm{ref}} = \sqrt{\frac{L_0}{C_0}};\ Z_{\mathrm{DUT}} = Z_0\sqrt{1 - j\frac{\zeta}{\kappa_0 Z_0}}$$

$$\kappa_0 = \kappa_{\mathrm{ref}} = \omega\sqrt{L_0 C_0};\ \kappa_{\mathrm{DUT}} = \kappa_0\sqrt{1 - j\frac{\zeta}{\kappa_0 Z_0}}$$

where L_0, C_0 are inductance and capacitance per unit length of the reference line and ζ the wall impedance per unit length seen by the beam.

For $\zeta \ll \kappa_0 Z_0$, one has

$$\frac{S_{21\mathrm{DUT}}}{S_{1\mathrm{ref}}} \approx e^{-j(\kappa_0 - \kappa_{\mathrm{DUT}})\ell}$$

and in further approximation one finds Walling's log-formula for the coupling impedance

$$Z = \zeta\ell \approx -2Z_0 \ln\frac{S_{21\mathrm{DUT}}}{S_{21\mathrm{ref}}}$$

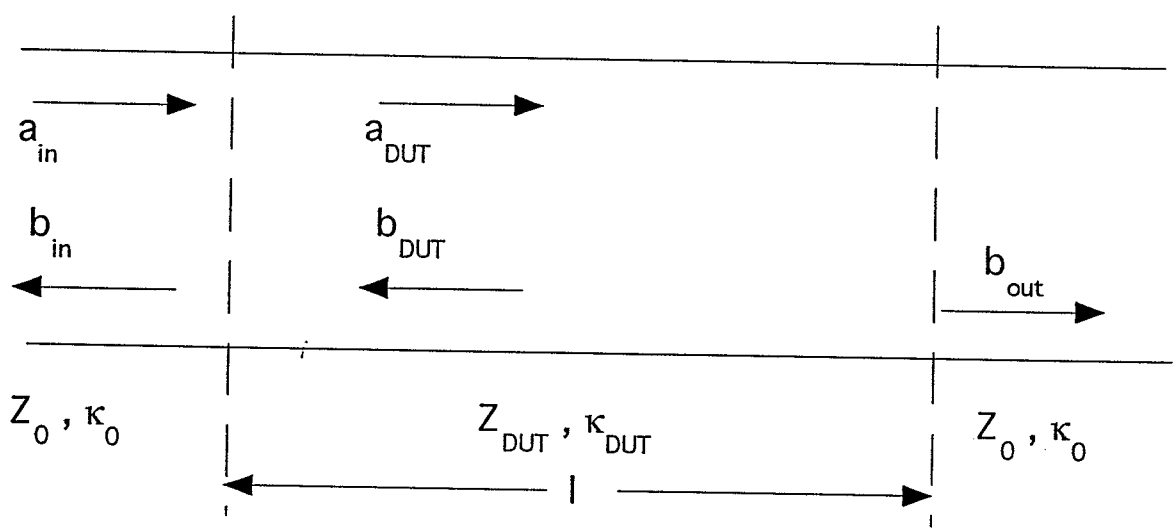

Fig. 19. Scattering waves in distributed impedance

The use of the log-formula approximation has been justified, and the limitation of the lumped-element formula has been demonstrated by comparing them in Fig. 20 with Nassibian's theoretical expressions for a travelling-wave kicker with characteristic impedance Z_C, propagation velocitiy v, and length ℓ

$$\begin{aligned} \mathrm{Re}Z &= \frac{1}{4} Z_C \left(1 - \cos \kappa_C \ell\right) \\ \mathrm{Im}Z &= \frac{1}{4} Z_C \kappa_C \ell \left(1 - \frac{\sin \kappa_C \ell}{\kappa_C \ell}\right) \\ &= \frac{1}{4} L_C \ell \omega \left(1 - \frac{\sin \kappa_C \ell}{\kappa_C \ell}\right) \end{aligned}$$

with

$$\kappa_C \ell = \frac{\omega \ell}{v} = \frac{L_C}{Z_C} \omega \ell$$

where L_C is the kicker inductance per unit length and $L_C \ell$ the total kicker inductance. Using the above exact expression for the forward scattering coefficient, one obtains the exat ratio $S_{21\mathrm{DUT}}/S_{21\mathrm{ref}}$ for Nassibian's impedance which then can be translated back into a coupling impedance via the lumped-element or log-formula approximation.

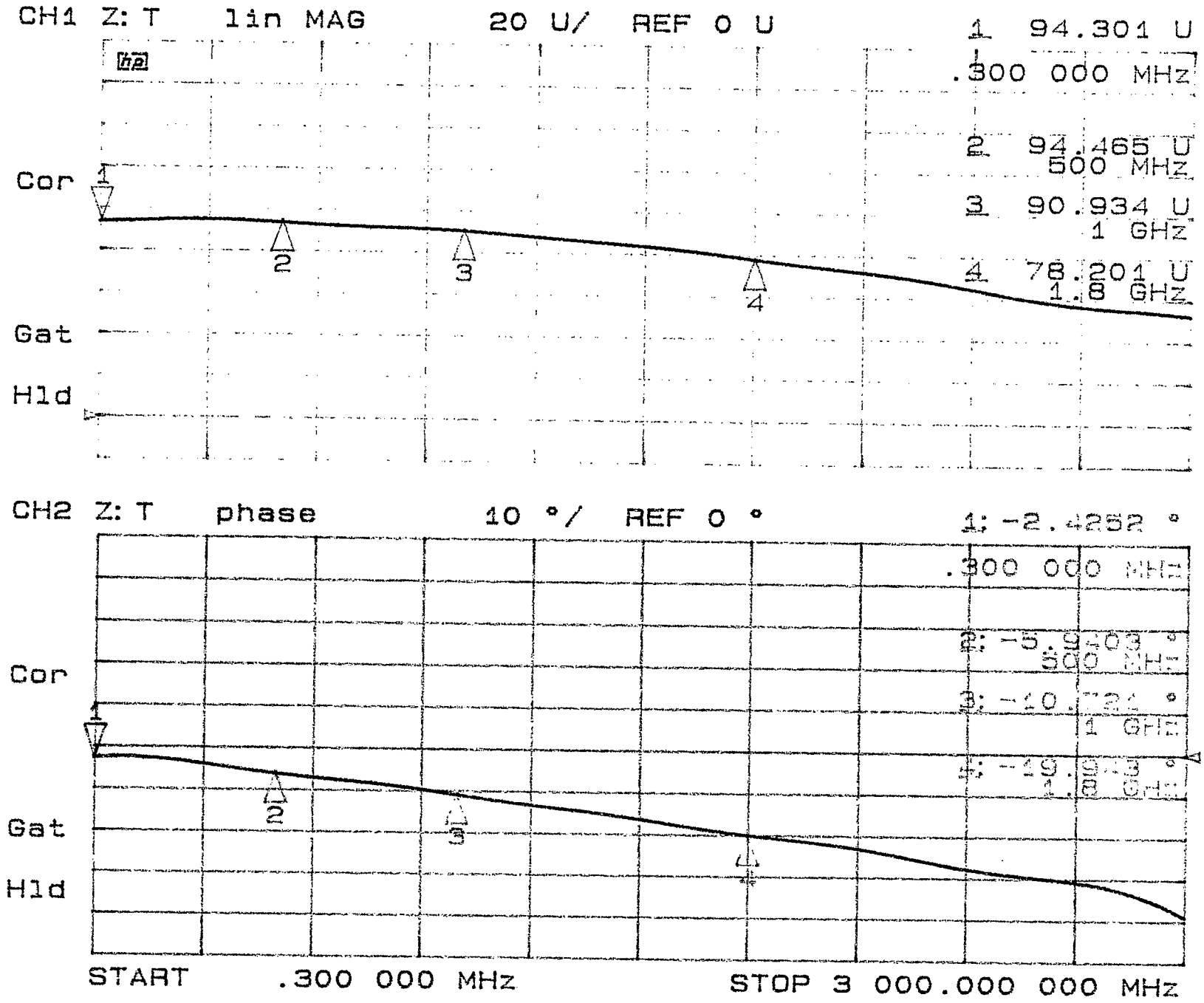

Fig. 17. Impedance of 100 Ω resistor from wire measurement

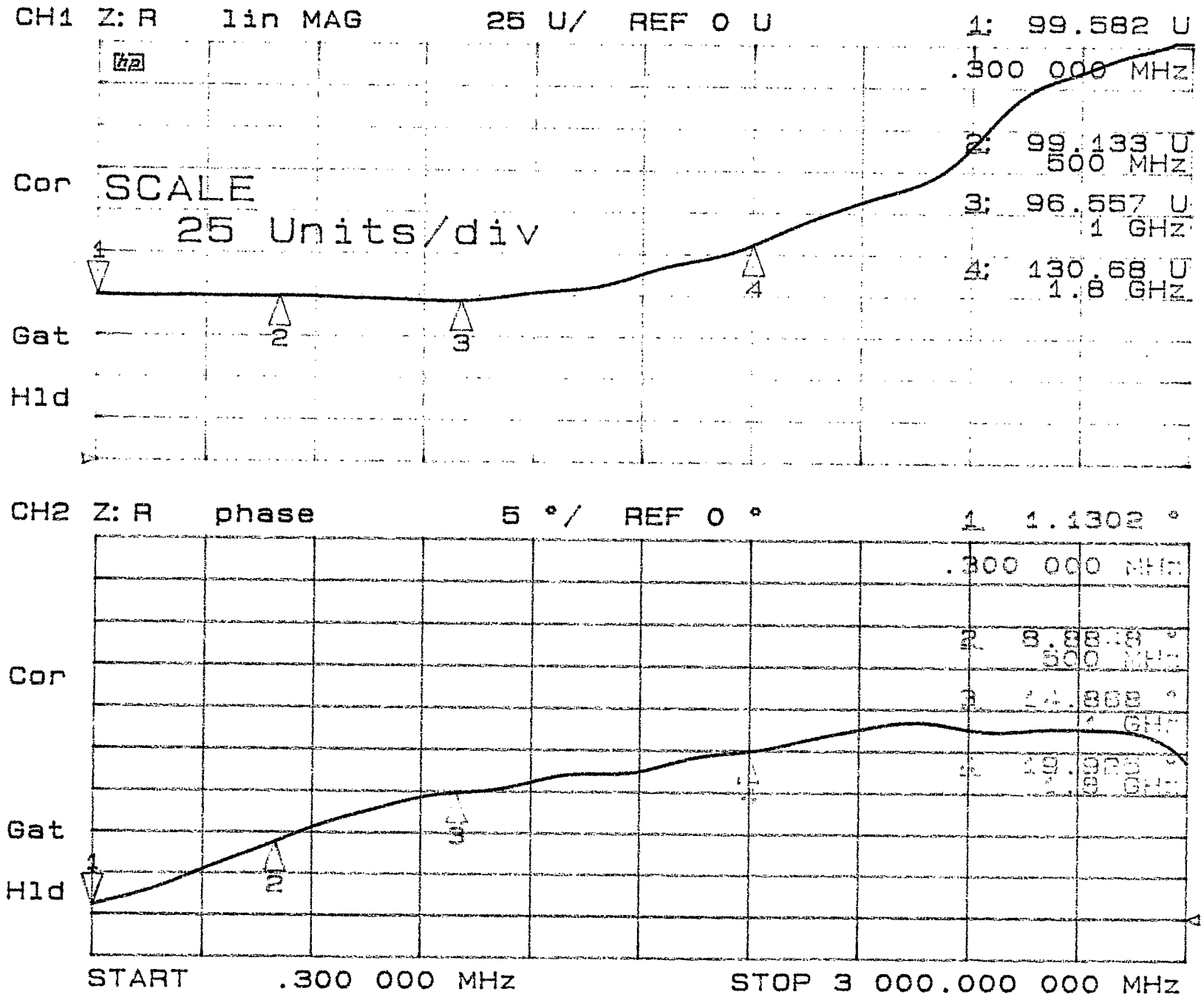

Fig. 18. Calibration of 100 Ω resistor

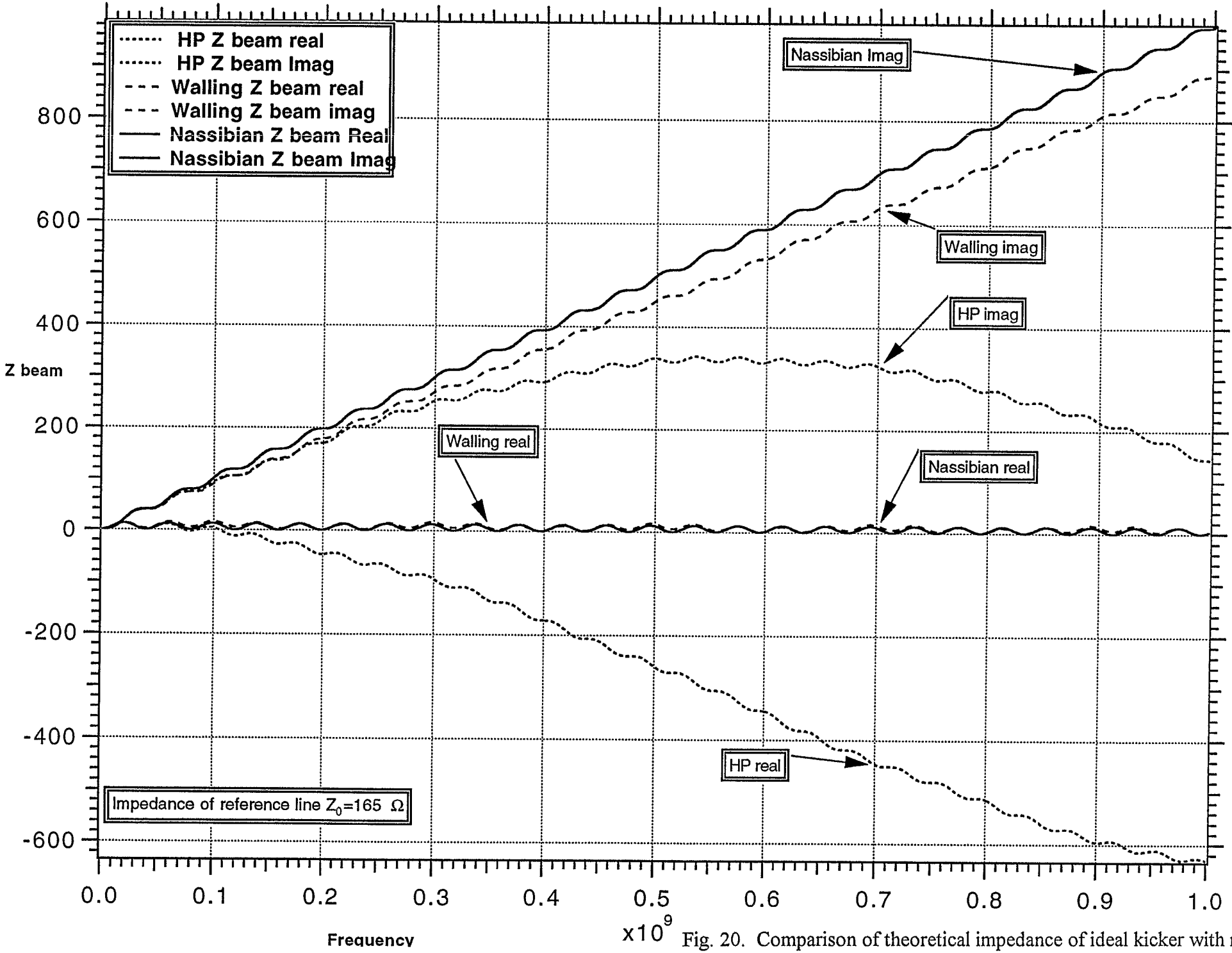

Fig. 20. Comparison of theoretical impedance of ideal kicker with results using the log and the lumped-element formulae

Appendix II: The Ferrite-Dominated Coupling Impedance

A particle beam traversing a structure such as the kicker will induce electromagnetic fields ("TM" or "E" modes) which are the source of the coupling impedance. The propagation velocity of the e.m. wave in the kicker is smaller than the particle velocity which represents a situation similar to shock waves or Cherenkov radiation. This effect was pointed out to us by Dome, who had analyzed the wake fields of relativistic particles in a dielectric lined circular wave guide.[10]

Such a situation can result in losses which are local and thus independent of the kicker termination. Consequently, the resulting coupling impedance cannot be obtained from Nassibian's analysis, which in essence treats the kicker as transformer.

A full analysis is beyond the scope of this report, but some qualitative aspects of this effect can be demonstrated by studying the simple case of a current sheet between ferrite blocks as shown in Fig. 21.

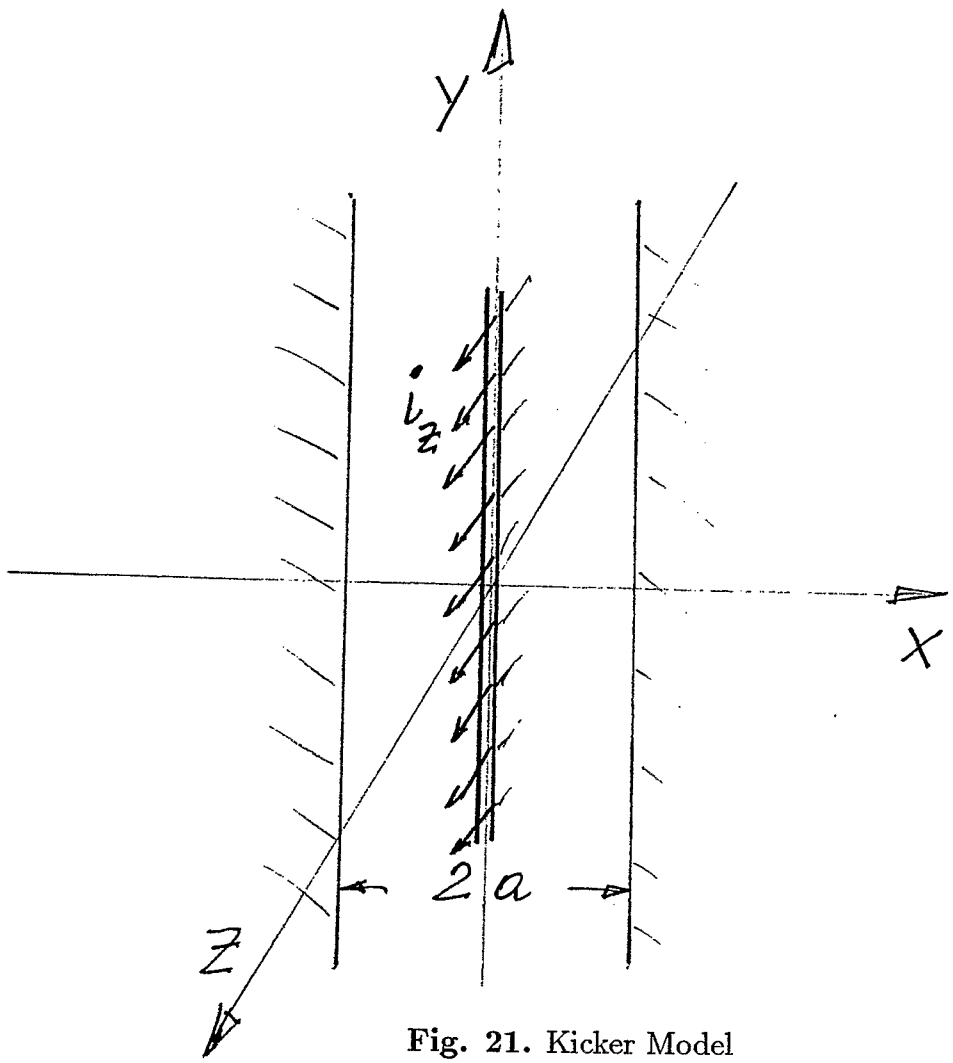

Fig. 21. Kicker Model

[10] G. Dome, Proc. 2nd EPAC, Nice 1990, p 628.

The electromagnetic/fields are generated by the current sheet with current density

$$i_Z = \frac{I}{2h} e^{-j\kappa z} e^{j\omega t}$$

where $\omega = v\kappa$ and h the vertical kicker height assuming $h \gg a$. The field expressions in the beam region are then given by (natural units $c = \mu_0 = 1$)

$$\begin{aligned}
E_x &= \frac{I}{vh} e^{-\xi x} - C_K \frac{\kappa}{\xi} \frac{\sinh \xi x}{\cosh \xi a} \\
E_y &= 0 \\
E_z &= j \frac{\left(1 - v^2\right) I \kappa}{vh\xi} e^{-\xi x} + j C_K \frac{\cosh \xi x}{\cosh \xi a} \\
H_x &= 0 \\
H_y &= \frac{I}{h} e^{-\xi x} + C_K \frac{\xi^2 - \kappa^2}{v\kappa\xi} \frac{\sinh \xi x}{\cosh \xi a} \\
H_z &= 0
\end{aligned}$$

with the common factor $e^{-j\kappa z} e^{j\omega t}$ suppressed and $\omega^2 = \kappa^2 - \xi^2$ or $\xi^2 = \left(1 - v^2\right) \kappa^2$.

The fields in the ferrite (ϵ, μ, σ) can be assumed to be independent in the left and right blocks as a result of the ferrite losses and induced eddy currents. One then finds $(x > a)$

$$\begin{aligned}
E_x &= -j C_F \frac{\kappa}{\xi_F} e^{-j\xi_F (x-a)} \\
E_y &= 0 \\
E_z &= j C_F e^{-j\xi_F (x-a)} \\
H_x &= 0 \\
H_y &= -j C_F \frac{\kappa^2 + \xi_F^2}{\mu v \kappa \xi_F} e^{-j\xi_F (x-a)} \\
H_z &= 0
\end{aligned}$$

with $\xi_F^2 = \left(\mu\epsilon v^2 - 1\right) \kappa^2 - j\mu\sigma v\kappa$. It follows that the fields penetrate the ferrite only to a "ferrite skin depth" of (assuming $\mu\epsilon \gg 1$ and $\sigma \ll \epsilon\omega$),

$$\delta_{\mathrm{F}} \approx \frac{2}{\sigma} \sqrt{\frac{\epsilon}{\mu}}$$

The "surface impedance" R_F of the ferrite is given by

$$R_F = -\left(\frac{E_2}{H_y}\right)_{x=a} = \frac{\xi_F}{\epsilon\omega - j\sigma}$$

and, if $\mu\epsilon \gg 1$,

$$R_{\mathrm{F}} \approx \sqrt{\frac{\mu\omega}{\epsilon\omega - j\sigma}}$$

As expected, this expression reduces in the case of very high conductivity ($\sigma \to \infty$) to the skin effect formula for metal,

$$R_F \sim \sqrt{\frac{j\mu\omega}{\sigma}}$$

and in the case of low loss ferrite to

$$R_F \sim \sqrt{\frac{\mu}{\epsilon}}\left(1 + j\frac{\sigma}{2\epsilon\omega}\right)$$

The induced field coefficients C_K and C_F are determined by field matching of E_z and H_y at the interface $x = a$. Of special interest is the ultrarelativistic limit, $v \sim 1$, where one finds

$$C_F = C_K = \frac{I}{h}\frac{R_F}{\omega a R_F - j}$$

The coupling impedance per unit length now follows as

$$Z = -\frac{1}{I}(E_z)_{x=0} = -j\frac{C_K}{I} = \frac{R_F}{h(1 + j\omega a R_F)}$$

It is to be noted that the impedance can be lossy even if the ferrite is not (however, the formula is only valid if the "ferrite skin depth" is smaller than the kicker height, $\delta_F \ll h$, which requires a lossy ferrite).